Structure and Expression of Hybrid Dysgenesis-Induced Alleles of the *ovarian tumor* (*otu*) Gene in *Drosophila melanogaster*

Georgette L. Sass,* J. Dawson Mohler,† Rosemary C. Walsh,* Laura J. Kalfayan* and Lillie L. Searles‡

**Department of Biochemistry and Biophysics, ‡Department of Biology, The University of North Carolina, Chapel Hill, North Carolina 27599-3280, and †Department of Biology, University of Iowa, Iowa City, Iowa 52240*

Manuscript received July 16, 1992
Accepted for publication October 5, 1992

ABSTRACT

Mutations at the *ovarian tumor* (*otu*) gene of *Drosophila melanogaster* cause female sterility and generate a range of ovarian phenotypes. Quiescent (QUI) mutants exhibit reduced germ cell proliferation; in oncogenic (ONC) mutants germ cells undergo uncontrolled proliferation generating excessive numbers of undifferentiated cells; the egg chambers of differentiated (DIF) mutants differentiate to variable degrees but fail to complete oogenesis. We have examined mutations caused by insertion and deletion of *P* elements at the *otu* gene. The *P* element insertion sites are upstream of the major *otu* transcription start sites. In deletion derivatives, the *P* element, regulatory regions and/or protein coding sequences have been removed. In both insertion and deletion mutants, the level of *otu* expression correlates directly with the severity of the phenotype: the absence of *otu* function produces the most severe QUI phenotype while the ONC mutants express lower levels of *otu* than those which are DIF. The results of this study demonstrate that the diverse mutant phenotypes of *otu* are the consequence of different levels of *otu* function.

DURING the initial stages of oogenesis in *Drosophila melanogaster*, a cystoblast, generated by a stem cell division, undergoes four mitotic divisions followed by incomplete cytokinesis to produce a sixteen-cell syncytium of cystocytes. This syncytium, surrounded by a layer of somatically derived follicle cells, differentiates into an egg chamber composed of fifteen nurse cells and an oocyte. During subsequent stages of oogenesis, materials needed to complete egg maturation and initiate embryogenesis are contributed to the developing oocyte by both nurse cells and follicle cells. A number of Drosophila genes are required for oogenesis, and mutations in these genes cause female sterility [see review by SPRADLING (1992)]. Of this group, the *ovarian tumor* (*otu*) gene is one of the best characterized in terms of genetic, morphological and molecular analyses.

Analysis of ovarian morphologies of 17 ethyl methanesulfonate (EMS)-induced mutant alleles has shown that *otu* mutations disrupt the proliferative and differentiation events of oogenesis (KING *et al.* 1986; STORTO and KING 1988). Mutant *otu* alleles result in a wide range of phenotypes, varying in severity from the absence of developing egg chambers to the production of apparently normal eggs. Typically, *otu* mutants are grouped into one of three phenotypic classes, depending on the predominant morphology of egg chambers. The most severe mutants belong to the quiescent (QUI) class and exhibit chamberless ovarioles with little or no apparent proliferation of germ cells. Mutants of the oncogenic (ONC) class are unable to control the cystocyte divisions and develop tumorous chambers containing excessive numbers of cells resembling cystocytes. Mutants of the differentiated (DIF) class exhibit variable degrees of nurse cell/oocyte differentiation but fail to complete oogenesis.

KING and STORTO (1988) proposed that the polymorphic ovarian phenotypes of *otu* mutants are the result of stage-specific blocks in oogenesis. In addition, morphological analysis of heteroallelic combinations representing the three phenotypic classes led to the prediction of two *otu* products (STORTO and KING 1987); molecular studies of *otu* have confirmed this prediction (STEINHAUER and KALFAYAN 1992). Two *otu* polypeptides are generated from alternatively spliced transcripts that differ only with respect to the inclusion of a small, 126-nucleotide exon. A 104-kD polypeptide is produced from transcripts that include this exon, and a 98-kD isoform is made when this exon is skipped. The otu proteins are localized in the cytoplasm of the nurse cells and the oocyte (STEINHAUER and KALFAYAN 1992). Germline transformation experiments have established that all *otu* functions are encoded within a 5-kb genomic DNA fragment (COMER, SEARLES and KALFAYAN 1992) which produces the alternatively spliced, ovary-specific *otu* transcripts.

Both the genetic and molecular analyses suggest that mutant *otu* alleles represent a hypomorphic series

in which the severity of a given allele is directly related to the level of *otu* function. The level of *otu* function might be altered by mutations that affect the activity or stability of otu proteins or by mutations affecting *otu* gene expression. However, the possibility has not been eliminated that the different phenotypes could be a consequence of altering different functional domains within the otu proteins. The *otu* mutations which have thus far been characterized molecularly were induced by EMS mutagenesis and affect protein coding sequences (STEINHAUER and KALFAYAN 1992). In this report, we have characterized a number of *P* element insertion mutations and deletion derivatives that affect *otu* expression. The four *P* insertion mutations, otu^{P1}, otu^{P2}, otu^{P3} and otu^{P4}, initially shown by Southern analysis to lie in the *otu* gene region (MULLIGAN, MOHLER and KALFAYAN 1988), have now been precisely mapped with respect to the *otu* transcription unit. Derivatives of the otu^{P3} and otu^{P4} alleles generated by hybrid dysgenic crosses have also been examined. This study examines the correlation between *otu* mutant phenotypes and *otu* expression levels.

MATERIALS AND METHODS

Fly stocks and culture conditions: Flies were reared on a standard cornmeal, yeast, and agar medium at 25° under a normal light-dark cycle. All *otu* mutants were maintained as balanced stocks, except otu^{P3} which was maintained as a homozygous stock. The deficiency *Df(1)RA2* which removes a portion of the *X* chromosome that includes the *otu* gene, is described in LINDSLEY and ZIMM (1992). The wild-type strain, Canton S, is also described in LINDSLEY and ZIMM (1992). The EMS-induced *otu* alleles used in this study are described in KING *et al.* (1986). Isolation of the four otu^{P} insertion mutants (otu^{P} alleles) was previously described by MULLIGAN, MOHLER and KALFAYAN (1988).

Generation of the otu^{P} derivatives: To identify fertile derivatives of sterile *P* element insertion alleles, males carrying either the otu^{P3} or otu^{P4} allele were mated to attached-*X* M strain females. The dysgenic male progeny were then mated to P strain females carrying *Df(1)RA2*, heterozygous with a nonrecombining *X* chromosome marked with *Bar* (*B*). F_1 female progeny, heterozygous for the dysgenic *X* chromosome and *Df(1)RA2*, were mated to their male siblings carrying the *B* marked *X* chromosome. Only revertant females produced progeny, and stocks of these fertile derivatives were established.

The otu^{P3} allele is sterile when heterozygous with *Df(1)RA2*, but is fertile when homozygous. To identify homozygous sterile derivatives of the otu^{P3} allele, F_1 female progeny heterozygous for the dysgenic and *B* marked *X* chromosomes were mated to their male siblings carrying the *B* marked *X* chromosome. The resulting F_2 female progeny which were heterozygous for the dysgenic and *B* marked *X* chromosome were mated to their male siblings which carried the dysgenic *X* chromosome. F_3 female progeny, homozygous for the dysgenic *X* chromosome and thus the altered otu^{P3} allele, were identified and tested for fertility. Stocks of sterile derivatives were established and shown to be *otu* alleles by complementation analysis with EMS-induced *otu* mutants.

Analysis of ovarian morphology: Ovaries from well-fed, 2–5-day-old flies were dissected in Ringer's solution (130 mM NaCl, 4.2 mM KCl, 2 mM $CaCl_2 \cdot 2H_2O$, and 10 mM HEPES, pH 6.9) and fixed with 2.5% glutaraldehyde in 50 mM PIPES (pH 7.4) for 15 min at room temperature. Following fixation, ovaries were incubated at 37° overnight in PBS (10 mM $Na \cdot PO_4$, pH 7.4, and 150 mM NaCl) containing 5 mM $K_3Fe(CN)_6$ and 5 mM $K_4Fe(CN)_6$. Ovarioles were teased apart and mounted in Aqua-Poly/Mount (Polysciences). Ovarioles were categorized and assigned to a phenotypic class as described in KING and RILEY (1982) and KING *et al.* (1986).

DNA analysis: Genomic DNA was prepared from adult flies as described in SCAVARDA and HARTL (1984). Southern blots were prepared (MANIATIS, FRITSCH and SAMBROOK 1982) and hybridized to cloned *otu* DNA fragments, labeled by random-priming (FEINBERG and VOGELSTEIN 1983). Clones of otu^{P1}, otu^{P3} and otu^{P4} used to identify *P* element insertion sites were generated in the following way. Genomic DNA was digested with *Eco*RI, and fragments of the expected size range [see MULLIGAN, MOHLER and KALFAYAN (1988)] were gel-purified and cloned into the *Eco*RI site of λgt10. The recombinant phage were packaged and the library was screened with a radiolabeled plasmid, p15-1, containing the 1.0-kb *Eco*RI fragment into which the *P* elements had inserted. Subsequently, *Eco*RI/*Hin*dIII fragments containing both *P* element and *otu* sequences were subcloned into M13mp8 and sequenced by the dideoxy chain termination method (SANGER, NICKLEN and COULSON (1977). The sequence was obtained from the *Hin*dIII site near the end of the *P* element and extended into flanking *otu* sequences. Regions of genomic DNA from otu^{P2} and all derivatives of the otu^{P3} allele (except the $otu^{P\Delta4}$ allele) were amplified by the polymerase chain reaction (PCR) (SAIKI *et al.* 1985) to generate substrates for sequencing. Briefly, the *otu* region to be sequenced was amplified from genomic DNA using *otu*-specific primers. Subsequently, single-stranded products were generated by a second round of asymmetric PCR with one of the original primers used in the double-stranded synthesis (KREITMAN and LANDWEBER 1989). The single-stranded templates were then sequenced using *otu*-specific primers and the Sequenase protocol (U.S. Biochemical Corp.).

RNA analysis: Total RNA was isolated from dissected ovaries of 2–6-day-old females as described previously (WAKIMOTO, KALFAYAN and SPRADLING 1986). Total RNA was fractionated on a 1% agarose gel containing 2.2 M formaldehyde and blotted to a nylon membrane as specified by the manufacturer (Amersham). Antisense ^{32}P-labeled riboprobes were generated as described by MELTON *et al.* (1984) using the plasmid pSP64-2.9, which contains the 3.2-kb *Eco*RI fragment of *otu* (MULLIGAN, MOHLER and KALFAYAN 1988) and the plasmid pGRP49, which contains *Drosophila melanogaster rp49* sequence (O'CONNELL and ROSBASH 1984). The nylon membranes were prehybridized at 60° for 6 h as described by COMER, SEARLES and KALFAYAN (1992). The blots were then hybridized overnight at 60° with 2×10^7 cpm of the *otu*-specific probe and 2×10^5 cpm of the *rp49*-specific probe. The blots were washed at room temperature in 2 × SSC, 0.5% SDS for 20 min and then at 65° in 0.2 × SSC, 0.5% SDS for 20 min.

Western analysis: Ovary extracts were prepared from 2–6-day-old females as described by STEINHAUER and KALFAYAN (1992). Ovary proteins were separated on 8% SDS-polyacrylamide gels (except where noted) and transferred to a PVDF membrane (ICN) using a semidry electrophoretic transfer apparatus (Bio-Rad). Blots were blocked for 1 hr in TBST [10 mM Tris-HCl (pH 8.0), 150 mM NaCl, 0.1% Tween-20] containing 5% non-fat dried milk. The blots were incubated with the primary antibody, anti-*otu* 670–811 described in STEINHAUER and KALFAYAN (1992), in TBST containing 1% non-fat dried milk overnight at 4°.

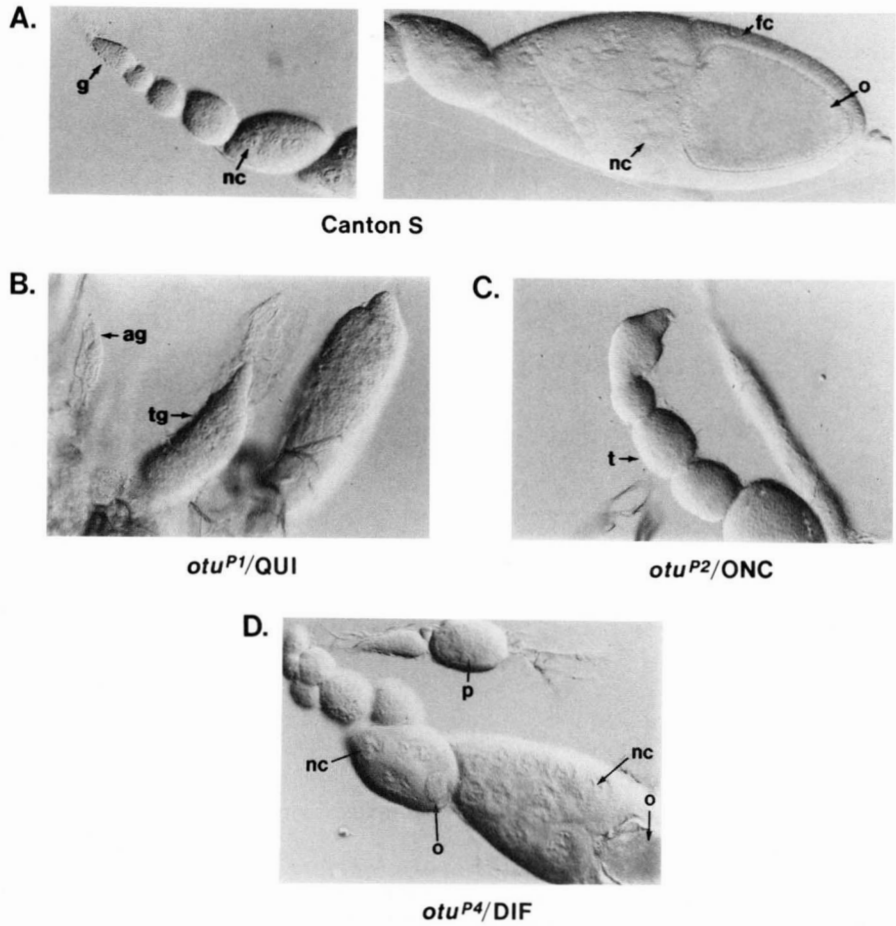

FIGURE 1.—Ovarian morphologies representing the phenotypic classes of *otu* mutants. The ovary of *D. melanogaster* is composed of a cluster of ovarioles, tube-like structures containing developing egg chambers. The initial stages of oogenesis take place in the germarium at the anterior end of the ovariole, and progressively more advanced chambers are found posteriorly. The two photographs in panel A illustrate the wild-type ovarian morphology showing the germarium (**g**) and developing egg chambers. A stage 10A egg chamber is shown on the right. The nurse cells (**nc**), follicle cells (**fc**), and oocyte (**o**) are indicated. Panel B illustrates the morphology of ovarioles seen in the chamberless QUI class. An agametic germarium (**ag**) which apparently lacks proliferating germ cells and a tumorous germarium (**tg**) with an excessive number of germ cells are indicated. Panel C shows tumorous chambers (**t**) contained within an ovariole belonging to the ONC class. In panel D, two types of ovarioles of the DIF class are shown. A chamber containing pseudonurse cells (**p**) and chambers containing both nurse cells (**nc**) and an oocyte (**o**) are shown. Some of these egg chambers have fewer or greater than the normal number of nurse cells. Pictures for all ovarian morphologies were taken using a 20× Nomarski objective.

Blots were washed four times for 5 min each in TBST and then incubated with an alkaline phosphatase-conjugated goat anti-rabbit secondary antibody (Promega), diluted 1:7,500 in TBST containing 1% non-fat dried milk for 1 h at room temperature. Blots were washed four times for 5 min each in TBST and then developed with 5-bromo-4-chloro-3-indolyl-phosphate (BCIP) and nitro blue tetrazolium (NBT) following the procedure suggested by the manufacturer (Bio-Rad). Blots used to detect otu protein were reprobed with a monoclonal anti-α-tubulin antibody (clone no. DM1A, Sigma) to control for loading differences. Blots were treated as described above except that the secondary antibody was a horseradish peroxidase-linked sheep anti-mouse antibody (Amersham), diluted 1:10,000, and blots were developed using the enhanced chemiluminescence detection system of Amersham.

RESULTS

Analysis of the *otu*^{P} alleles: Four *otu*^{P} alleles were recovered in a hybrid dysgenesis screen as female sterile mutations uncovered by a deficiency, *Df(1)RA2*, which removes the *otu* gene (MULLIGAN, MOHLER and KALFAYAN 1988). The ovarian morphologies of the *otu*^{P} alleles were examined; wild-type and representative mutant ovarioles are shown in Figure 1. Ovaries of females carrying the *otu*^{P1} allele contain predominantly quiescent ovarioles (Table 1A). The quiescent ovarioles are of two types: ovarioles containing a germarium with apparently no mitotically active germ cells (agametic germarium, Figure 1B) and those with an excessive number of germ cells (tumorous germarium, Figure 1B). In addition, *otu*^{P1} occasionally produces tumorous ovarioles (Table 1A). Because of the predominance of quiescent ovarioles, the *otu*^{P1} allele was reassigned to the more severe QUI phenotypic class rather than the ONC class designation of MULLIGAN, MOHLER and KALFAYAN (1988). The *otu*^{P2} allele produces a significant percentage of tumorous ovarioles and was placed in the ONC class (Table 1A).

TABLE 1

QTPO scores and phenotypic class of *otu* mutations

Allele	Scores[a] Q	T	P	O	Phenotypic class[b]
A. Insertion					
otu^{P1}	83	15	2	0	QUI
otu^{P2}	33	47	15	5	ONC
otu^{P3}	0	3	11	86	DIF
otu^{P4}	0	8	12	80	DIF
B. Deletion					
$otu^{P\Delta1}$	79	21	0	0	QUI
$otu^{P\Delta4}$	100	0	0	0	QUI
$otu^{P\Delta6}$	94	6	0	0	QUI
$otu^{P\Delta3}$	15	84	1	0	ONC
$otu^{P\Delta2}$	0	8	22	70	DIF
$otu^{P\Delta5}$	2	11	39	48	DIF

[a] QTPO scores were determined as described in KING *et al.* (1986) and represent the percentage of ovarioles which are chamberless (Q), tumorous (T), contain differentiated nurse cells without an oocyte (P), or contain a nurse cell/oocyte syncytium (O). An average of 8 ovaries (100 ovarioles) were examined for each allele.

[b] The QUI phenotypic class is characterized by high Q values, the ONC class by high T values and the DIF class by high P and O values.

A tumorous ovariole is composed of chambers that contain large numbers of undifferentiated germ cells (Figure 1C). The otu^{P3} and otu^{P4} alleles belong to the DIF class (Table 1A). In Figure 1D, two ovarioles from the otu^{P4} DIF allele illustrate both types of ovarioles characteristic of a DIF mutant: those with chambers lacking an oocyte but containing nurse cells (pseudonurse cells) and those with a nurse cell/oocyte syncytium.

Previously, the *P* element insertions in the otu^{P} mutants were mapped to the 1.0-kb *Eco*R1 genomic fragment of the *otu* gene (MULLIGAN, MOHLER and KALFAYAN 1988). In this study, we have precisely mapped these insertions with respect to the *otu* transcription unit. Transcription of the *otu* gene, which lacks a TATA box, initiates at several sites spread over a 62-bp region (COMER, SEARLES and KALFAYAN 1992). Sequence analysis of the otu^{P} alleles revealed that the *P* element insertion sites are clustered within a region upstream of the major transcription start sites and downstream of two minor transcription start sites (Figure 2). The *P* elements in otu^{P1}, otu^{P2} and otu^{P4} are inserted at exactly the same position, between 14 and 15 bp upstream of the first major transcription start site, designated as +1 by COMER, SEARLES and KALFAYAN (1992). The target site duplication GGCTAGAT, located from −14 to −7, is found at both ends of the insertions and matches the consensus target sequence GGCCAGAC (O'HARE and RUBIN 1983) at six of the eight positions. The *P* element in the otu^{P3} allele inserted 6 bp downstream of the other insertions, at the target sequence GGCGCGAT (−1 to −8). This target sequence is also duplicated and matches the consensus sequence at five out of eight base pairs. Thus, all of the insertions lie within a short distance upstream of the major transcription start sites.

The sizes of the *P* element insertions were deduced from Southern analysis (data not shown) (MULLIGAN, MOHLER and KALFAYAN 1988) and are indicated in Figure 2. The otu^{P1} QUI allele contains an apparently full-length 2.9-kb *P* element in the opposite transcriptional orientation (antisense orientation) as the *otu* gene. The otu^{P2} ONC allele contains a 2.0-kb *P* element that is in the same transcriptional orientation (sense orientation) as the *otu* gene. The otu^{P4} DIF allele has a 0.5-kb *P* element in an antisense orientation. The otu^{P3} DIF allele contains a 0.6-kb *P* element in the sense orientation, but inserted at a different site as noted above. Thus, the two alleles with larger insertions result in the more severe QUI and ONC phenotypes, and the smaller insertions produce a DIF phenotype.

Northern analysis of the DIF alleles otu^{P3} and otu^{P4} indicates that these alleles express *otu* transcripts that are the same size as those seen in wild type (Figure 3). This suggests that insertion of a *P* element at either of the sites does not interfere with initiation of transcription. However, the level of expression in these alleles is reduced with the otu^{P4} allele being affected to a greater extent than the otu^{P3} allele.

The effect of *P* element insertions on the level of otu protein accumulation in the otu^{P} alleles was examined by Western analysis (Figure 4). In wild-type adult ovaries, otu protein is relatively abundant, and the two otu isoforms show an unequal distribution, the 98-kD isoform being more abundant than the 104-kD isoform (Figure 4, lanes 1 and 5) (STEINHAUER and KALFAYAN 1992). The otu^{P1} QUI allele does not produce detectable levels of otu protein (Figure 4, lane 2). The otu^{P2} ONC mutant was found to accumulate reduced levels of otu protein, and only the 104-kD otu isoform was observed (Figure 4, lane 6). This pattern of accumulation, *i.e.*, the predominance of the 104-kD isoform, has also been observed in other female-sterile mutations which produce a tumorous phenotype and in ovaries enriched for the predifferentiated stages oogenesis (G. SASS, unpublished results). These observations indicate that the presence of only the 104-kD isoform is a consequence of the state of tissue differentiation. Other experiments (A. COMER, unpublished results) have shown that the absence of the 98-kD otu isoform does not produce an ONC phenotype. Both otu isoforms are present in the otu^{P3} and otu^{P4} DIF mutants, although at reduced levels relative to wild type (Figure 4, lanes 3, 7 and 4). The reduced level of otu protein and RNA accumulation seen in otu^{P4} relative to the homozygous fertile otu^{P3} DIF mutant supports the categorization of otu^{P4} as a more severe DIF allele as initially

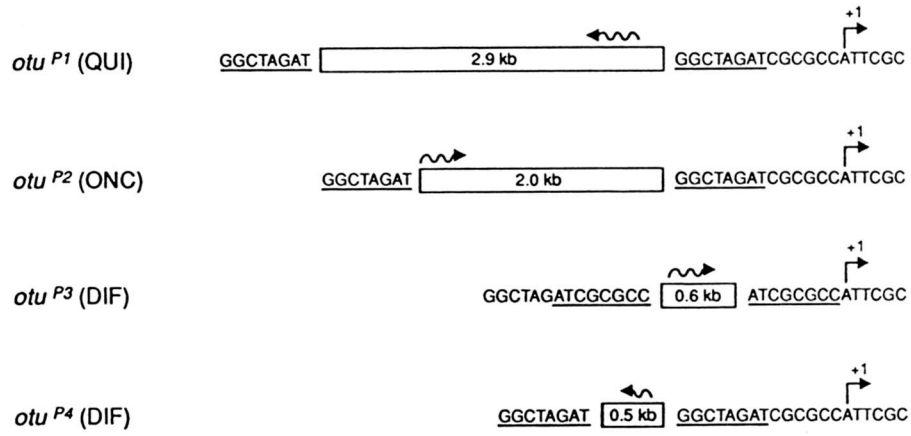

FIGURE 2.—Molecular structure of the *otu*^{P} alleles. The size, orientation and site of insertion is shown for the four alleles examined. The size of each *P* element shown in the open box was determined by Southern analysis (data not shown). The direction of *P* element transcription is indicated by a wavy arrow above the open box and was determined by both Southern and sequence analysis. The 8-bp target sequence which is duplicated during *P* element insertion is underlined. The first major transcription start site is labeled +1 and is equivalent to genomic position 664 in STEINHAUER, WALSH and KALFAYAN (1989).

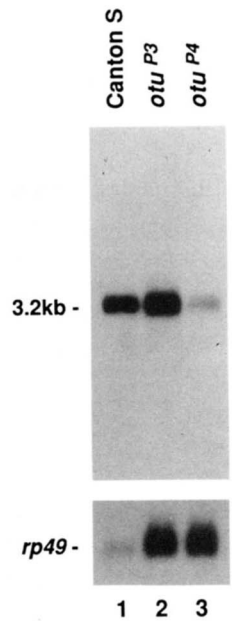

FIGURE 3.—Analysis of *otu* transcripts expressed in *otu*^{P3} and *otu*^{P4}. Total RNA was isolated from adult ovaries and analyzed by Northern blot hybridization using an *otu*-specific riboprobe. Lane 1 contains 2.5 μg of Canton S RNA and lanes 2 and 3 contain 20 μg of *otu*^{P3} and *otu*^{P4} RNA, respectively. The lower panel shows the same blot probed with *rp49* sequences to control for loading differences.

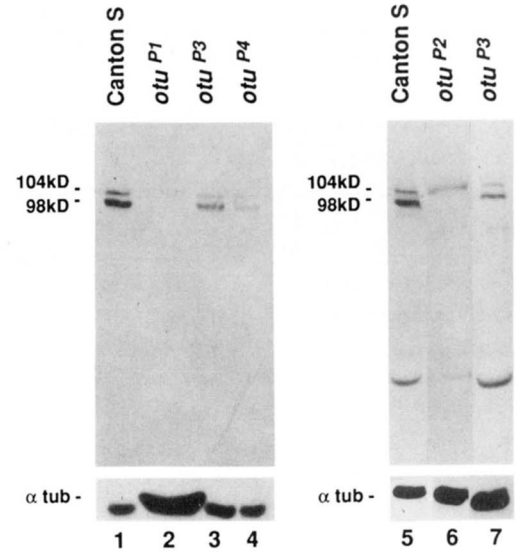

FIGURE 4.—Analysis of otu protein accumulation in *otu*^{P} alleles. Ovary extracts were prepared from Canton S and *otu* mutants. Canton S (25 μg) is shown in lanes 1 and 5, the *otu*^{P1} QUI allele (100 μg) in lane 2, the *otu*^{P2} DIF allele (100 μg) in lane 6, the *otu*^{P3} DIF allele (50 μg) in lanes 3 and 7, and the *otu*^{P4} DIF allele (50 μg) in lane 4. The position and corresponding molecular weights of the two *otu* isoforms are indicated. The extra bands seen in the blot containing the *otu*^{P2} DIF allele represent a protein which cross-reacts with our antibody and is not related to the otu proteins. The lower panels show the same blots probed with α-tubulin antibody as a control for loading and/or transfer differences.

suggested by complementation studies (MULLIGAN, MOHLER and KALFAYAN 1988).

Analysis of fertile derivatives of the *otu*^{P3} allele: Revertants of the *otu*^{P3} and *otu*^{P4} alleles were analyzed molecularly (Figure 5, A and B). Three *otu*^{P3} revertants (*otu*^{PR4A}, *otu*^{PR7} and *otu*^{PR9}) appeared to have lost the *P* element by Southern analysis (data not shown). Sequence analysis of the revertant *otu*^{PR4A} indicates that the *P* element was precisely excised. However, sequence analysis of the revertants, *otu*^{PR7} and *otu*^{PR9}, showed that *P* element excision was not precise and that these revertants retained 35 and 32 bp, respectively, of the *P* element terminal inverted repeat sequence. Southern analysis of a fourth *otu*^{P3} revertant, *otu*^{PR5}, showed that this derivative has a smaller insertion (0.4 kb) than that of the parental allele, and it is in the opposite orientation as the original insertion. Thus, this revertant does not appear to be the result of internal deletion of *P* element sequences but rather the replacement of the original element with a different, smaller *P* element. Similar events have been de-

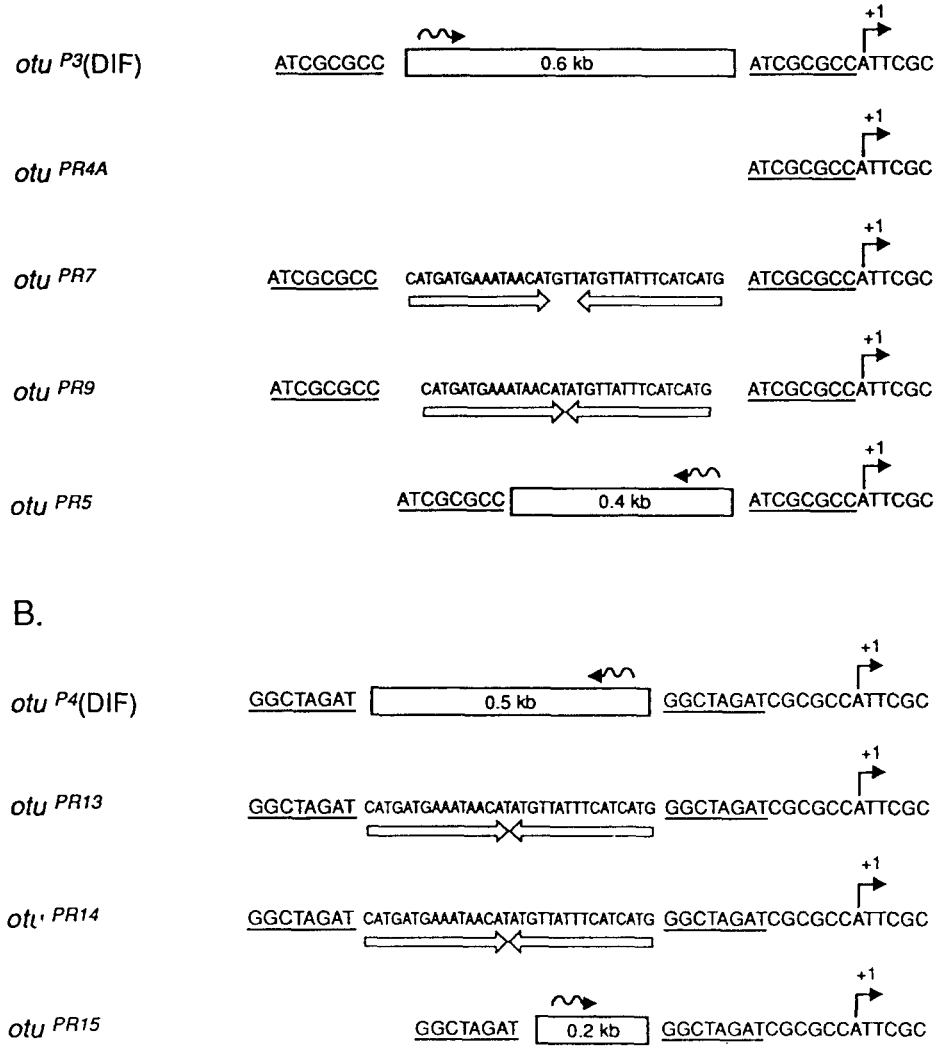

FIGURE 5.—Molecular structure of the fertile derivatives of the otu^{P3} and otu^{P4} alleles. Panels A and B show the DNA sequence of fertile derivatives of the otu^{P3} and otu^{P4} DIF alleles, respectively, in the region of the *P* element insertion. The size of each *P* element is shown in the open box, direction of *P* element transcription is indicated by a wavy arrow above the open box, and the 8-bp target site duplication is underlined. The otu^{PR4A} allele is a precise excision of the *P* element. Sequence of the derivatives otu^{PR7}, otu^{PR9}, otu^{PR13} and otu^{PR14} are shown with residual *P* element inverted repeat sequences indicated by an open arrow. The size of the *P* element in the otu^{PR5} and otu^{PR15} derivatives was determined by Southern analysis, and the flanking region was sequenced.

scribed previously (GEYER *et al.* 1988; WILLIAM, PAPPU and BELL 1988).

Three otu^{P4} revertants were similarly examined (Figure 5B). Two of these revertants, otu^{PR13} and otu^{PR14}, retain 32 bp of the *P* element terminal inverted repeat sequence and both are identical to otu^{PR9}. The otu^{PR15} revertant appears to be another example of a *P* element replacement because the revertant contains a smaller insertion (0.2 kb) compared to 0.5 kb in the original mutant, and the insertion is in the opposite orientation as the otu^{P4} insertion. Thus, for each of these revertants, the restoration of fertility is associated with the elimination or reduction in the size of the *P* element insertions. The fact that reversion does not require precise excision of the transposon indicates that the mutant phenotypes of the parental alleles are not due to the disruption of specific *otu* sequences at the insertion sites.

Western analysis of ovary extracts from the otu^{PR} alleles shows that restoration to fertility in the otu^{P} derivatives is a direct consequence of increased expression of *otu* (Figure 6). All revertants express wild type levels of both otu isoforms including the revertants, otu^{PR5} and otu^{PR15}, which contain smaller *P* elements. Thus, a reduction in the size of the insertion is sufficient to restore expression to wild-type levels.

Analysis of sterile, deletion derivatives of the otu^{P3} allele: Females carrying the otu^{P3} allele are fertile as homozygotes. A hybrid dysgenic cross was used to generate female-sterile deletion derivatives, designated $otu^{P\Delta}$. The productivity of these deletion derivatives when heterozygous with other *otu* mutations was examined (Table 2) and was initially used to rank these mutants in order of severity. Analysis of ovarian morphology showed that this scheme generated mutants representing each of the *otu* phenotypic classes (Table 1B).

The predominance of quiescent ovarioles in the deletion mutants $otu^{P\Delta 1}$, $otu^{P\Delta 4}$ and $otu^{P\Delta 6}$ placed these alleles in the QUI class (Table 1B). As described for otu^{P1}, the quiescent ovarioles in $otu^{P\Delta 1}$ and $otu^{P\Delta 6}$ contain both agametic and tumorous germaria. These

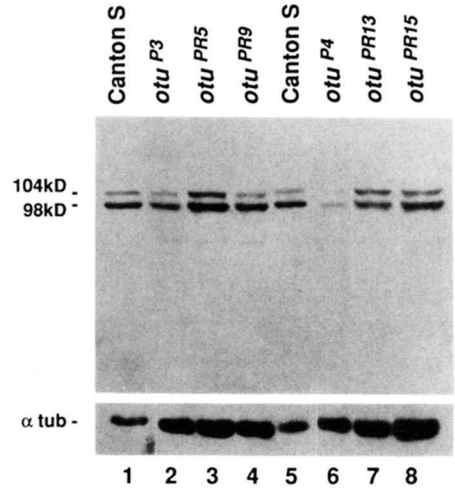

FIGURE 6.—Levels of otu protein accumulation in fertile derivatives of the otu^{P3} and otu^{P4} alleles. In each lane, 50 μg of ovary extract was loaded for analysis by Western blot. Canton S is shown in lanes 1 and 5. otu^{P3} and two of its fertile derivatives, otu^{PR5} and otu^{PR9} are shown in lanes 2, 3 and 4, respectively. otu^{P4} and fertile derivatives otu^{PR13} and otu^{PR15} are shown in lanes 6, 7 and 8, respectively. The lower panel shows the same blot probed with α-tubulin antibody as a control for loading and/or transfer differences.

TABLE 2

Productivity of heterozygotes

Allele	*Df(1)RA2*	otu^{P3}	EMS-QUI[a]	EMS-ONC[b]
otu^{P3} (DIF)	−	++++	++++	++++
$otu^{P\Delta2}$ (DIF)	−	+++	−	++
$otu^{P\Delta5}$ (DIF)	−	+++	−	++
$otu^{P\Delta3}$ (ONC)	−	++	−	+
$otu^{P\Delta6}$ (QUI)	−	++	−	+
$otu^{P\Delta4}$ (QUI)	−	+	−	−
$otu^{P\Delta1}$ (QUI)	−	+	−	−

Each $otu^{P\Delta}$ allele was crossed to *Df(1)RA2*, otu^{P3}, three EMS-induced QUI alleles and two EMS-induced ONC alleles, and the productivity of heterozygous females determined. Productivity was measured as the percentage of progeny produced by an $otu^{P\Delta}$ allele relative to the parental otu^{P3} allele when heterozygous. Each + represents a value in the range of 25%.

[a] EMS-QUI refers to the otu^{2}, otu^{10} or otu^{17} alleles.

[b] EMS-ONC refers to the otu^{11} or otu^{13} alleles.

alleles also generate some tumorous ovarioles. On the other hand, $otu^{P\Delta4}$ allele was found to produce only quiescent ovarioles, and these in turn appeared to contain mostly agametic germaria.

The QUI alleles have deletions of functional regions of the *otu* gene as determined by Southern analysis. The deletion in the $otu^{P\Delta1}$ allele is approximately 10 kb, removing the entire protein coding region of *otu* (Figure 7A). Sequence analysis demonstrated that the upstream breakpoint of this deletion is within the upstream inverted repeat of the *P* element (data not shown). The deletion extends downstream into the chorion gene cluster (data not shown). Consistent with deletion of chorion gene sequences are complementation studies which indicate that $otu^{P\Delta1}$ fails to complement mutations of the S38 and S36 chorion genes (D. MOHLER, unpublished results). The deletion in the $otu^{P\Delta4}$ QUI allele is approximately 2.6 kb and removes sequences both upstream and downstream of the *P* element insertion site (Figure 7A). The deletion removes the entire 1.0 kb *otu* *Eco*RI fragment and approximately 100 bp of DNA upstream of this fragment. The downstream deletion endpoint is within the coding region of *otu*. Thus, the entire *otu* regulatory region and a portion of the coding region are deleted in this mutant. In the third QUI derivative, $otu^{P\Delta6}$, a 1.6-kb deletion removes most of the *P* element and 1 kb of flanking upstream sequence (Figure 7A). Sequence analysis of this deletion demonstrated that the downstream target site duplication and 14 bp of the *P* element inverted repeat remain (Figure 7B). The adjacent upstream sequence does not match known sequences, presumably because it is derived from a region that extends beyond that previously sequenced. The major transcription start sites have not been deleted in this mutant, and the coding region is unaffected; however, the deletion removes all of the known *otu* upstream regulatory sequences.

The $otu^{P\Delta3}$ mutant produces an ONC phenotype with an unusually high proportion of tumorous ovarioles (see Table 1B). Southern and DNA sequence analyses showed that this allele has a 437 bp deletion with exactly the same downstream endpoint as the $otu^{P\Delta6}$ QUI allele; both retain the same 14-bp sequence of the inverted repeat (Figure 7, A and B). However, the $otu^{P\Delta3}$ deletion does not extend as far upstream. The upstream boundary of the deletion is at position −446. Therefore, like $otu^{P\Delta6}$, this deletion removes all known *otu* upstream regulatory sequences. Yet, the less severe phenotype of $otu^{P\Delta3}$ relative to $otu^{P\Delta6}$ indicates a difference in the efficiency of expression of these two *otu* alleles. Perhaps the phenotypic differences between these two mutants are a consequence of position effects produced by the juxtaposition of different sequences upstream of the *otu* transcription unit.

The $otu^{P\Delta2}$ and $otu^{P\Delta5}$ alleles were assigned to the DIF class (Table 1B). Ovarioles examined in the deletion DIF derivatives were very similar to those from the insertion DIF alleles in that most of the ovarioles contained differentiated chambers. However, these mutants have a higher proportion of ovarioles containing the more severe DIF chambers that lack an oocyte.

The $otu^{P\Delta2}$ DIF and $otu^{P\Delta5}$ DIF alleles were isolated independently, but are identical as determined by sequence analysis (Figure 7B). The DNA of these alleles has 16 bp of the upstream *P* element inverted repeat, followed by a short stretch (13 bp) of sequence of unknown origin, which may have been generated by gap repair during the deletion event (see O'HARE

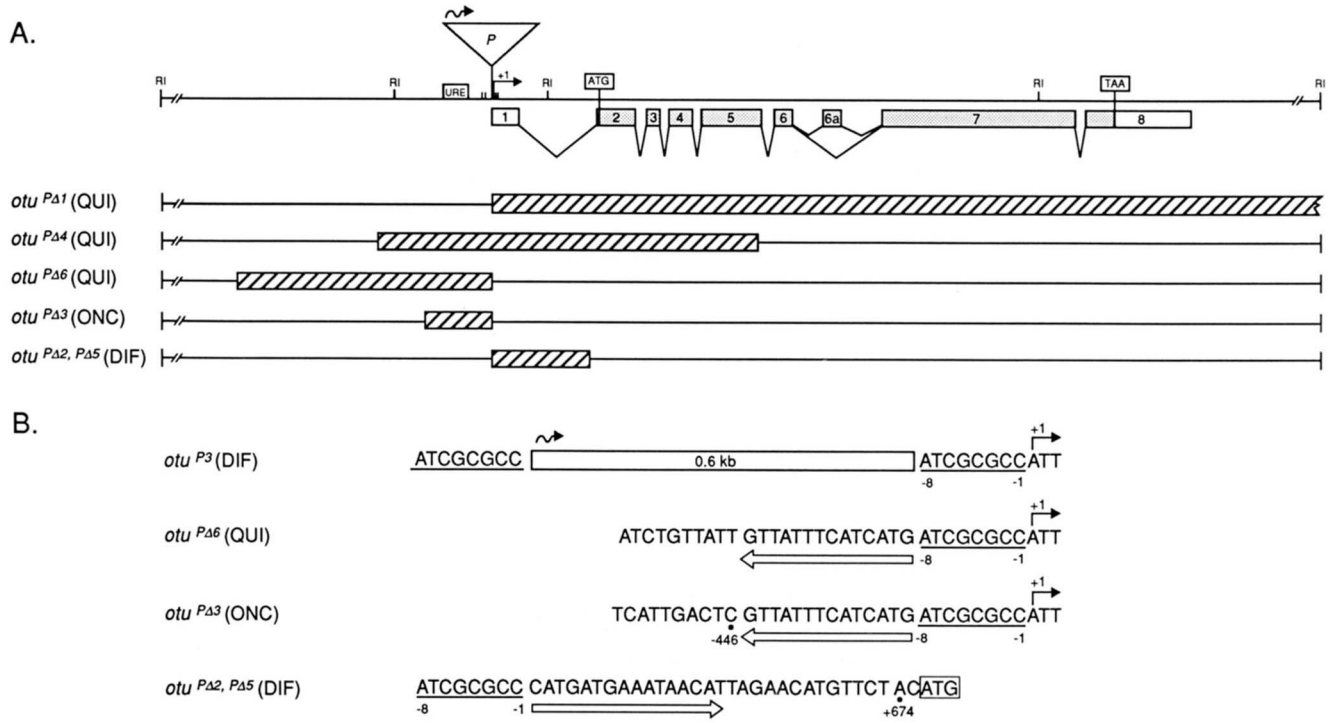

FIGURE 7.—Molecular structure of deletion derivatives of the otu^{P3} DIF allele. Panel A shows the deleted regions as boxes containing diagonal lines. The insertion site of the *P* element in otu^{P3} is represented as an inverted triangle. Transcription start sites are indicated by vertical lines on the restriction map of the *otu* gene. The first major transcription start site is indicated by +1 and a previously identified upstream regulatory region is shown as an open box labeled URE (COMER, SEARLES and KALFAYAN 1992). The intron/exon structure is illustrated beneath the restriction map of the *otu* region. The alternative splicing event (splicing of alternate exon 6A) which generates the 98- or 104-kD isoform is depicted. The translation initiation and stop codons are shown. In panel B, the sequences of the region surrounding the deletion breakpoints in $otu^{P\Delta6}$, $otu^{P\Delta3}$, $otu^{P\Delta2}$ and $otu^{P\Delta5}$ are shown. The 8-bp target site duplication is underlined. The residual portion of the inverted terminal repeat of the *P* element is indicated by an open arrow beneath the sequence. In the cases where *otu* sequence at a deletion breakpoint is known, the nucleotide is marked with a •, and its position relative to the first major transcription start site is indicated.

and RUBIN 1983). The downstream end point of the deletion is at +674 in the *otu* gene. Thus, this 673-bp deletion removes the major transcription start sites and the entire transcribed leader region, including the presumed translational start codon (Figure 7A). Upstream regulatory sequences and the minor transcription start sites are intact in these derivatives. Furthermore, an alternative in-frame translational start codon, the third codon in the wild-type gene, is present in these alleles. Presumably, these remaining regulatory signals are sufficient to direct a reduced level of *otu* gene activity.

Ovary extracts prepared from $otu^{P\Delta2}$, $otu^{P\Delta3}$ and $otu^{P\Delta5}$ were examined by Western analysis (Figure 8). The $otu^{P\Delta3}$ ONC allele expresses the 104-kD isoform at a significantly reduced level compared to wild type (Figure 8, lane 2). This pattern of protein accumulation was also observed in the other ONC mutant otu^{P2} (see Figure 4, lane 6), and as described earlier, the presence of only the 104-kD isoform is a consequence of the state of tissue differentiation. The $otu^{P\Delta2}$ and $otu^{P\Delta5}$ DIF alleles express both otu isoforms but at reduced levels relative to wild type (Figure 8, lanes 4 and 5), and the levels are similar to that seen in the otu^{P4} DIF mutant.

DISCUSSION

Structural changes in the *otu* gene affect levels of expression: We have analyzed four *otu* mutant alleles that have *P* element insertions clustered together in a small region, near the 5′ end of the gene. Three of the *P* elements inserted at precisely the same site, 15 bp upstream of the first major transcription start site, and the fourth *P* element inserted into a site located 6 bp downstream of the other transposons. The insertions in these positions do not appear to significantly affect the transcription initiation from the major start sites, since the transcripts produced from these mutants are the same size as wild type. Perhaps this is because sequences that control initiation at these sites within the TATA-less *otu* promoter are located in the transcribed leader region as has been shown for other Drosophila promoters that lack a TATA box [see, for example, BIGGIN and TJIAN (1988) or PERKINS, DAILEY and TJIAN (1988)]. We suggest that the *P* elements disrupt *otu* expression by increasing the distance between regulatory signals near the transcription start sites and upstream elements required for normal levels of expression. An essential regulatory region has been mapped between −310 and −190 of

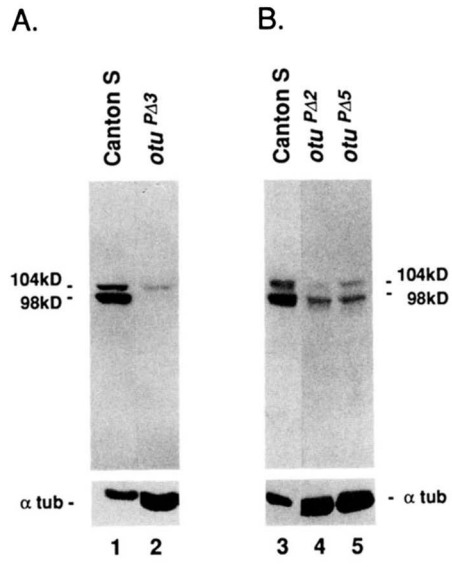

FIGURE 8.—Western analysis of ovary extracts from several otu^{P3} deletion derivatives $otu^{P\Delta3}$, $otu^{P\Delta2}$ and $otu^{P\Delta5}$ by Western blot. In panel A, lane 1 contains Canton S (50 μg) and lane 2 contains $otu^{P\Delta3}$ ONC allele (100 μg). In panel B, Canton S (50 μg) is shown in lane 3 and the DIF alleles $otu^{P\Delta2}$ and $otu^{P\Delta5}$ (90 μg each) are in lanes 4 and 5, respectively. The lower panels show the same blots probed with α-tubulin antibody as a control for loading and/or transfer differences. The samples in panels A and B were resolved on 8% and 5% polyacrylamide gels, respectively.

the wild-type *otu* gene (COMER, SEARLES and KALFAYAN 1992), and presumably sequences in this region are bounded by one or more specific transcriptional activators. Studies of transcriptional activation indicate that certain activators that function properly when bound to sites located within a few hundred base pairs of the transcription start site are ineffective when bound at more distant sites [see review by PTASHNE (1986)].

Consistent with this hypothesis is the observation that the severity of the *otu* mutant phenotypes and the level of expression produced by these insertions correlate with the size of the *P* element inserted rather than the orientation or position of the insertions. The least severe alleles, otu^{P3} and otu^{P4}, exhibit a DIF phenotype and contain relatively small *P* element insertions, 0.6 and 0.5 kb, respectively. The level of expression in these alleles is reduced relative to wild type. Expression is further reduced in the otu^{P2} ONC and otu^{P1} QUI alleles which have larger insertions (2.0 and 2.9 kb, respectively). The smaller otu^{P2} insertion allows a low level of expression while the larger otu^{P1} insertion apparently eliminates expression.

The restoration of *otu* gene activity in the fertile derivatives of otu^{P3} and otu^{P4} in every case can be correlated with a decrease in the size of the *P* element insertion. Several of these revertant alleles have residual *P* element sequences remaining, and yet they accumulate wild-type levels of *otu* products. This observation provides evidence that the disruption of specific sequences at the *P* element insertion sites is not the cause of the mutant phenotypes. However, not all of the observed effects can be explained on the basis of the insertion size. For example, genetic and Western blot analyses indicate that the otu^{P3} allele has a higher level of expression than otu^{P4}; however, the otu^{P3} insertion is slightly larger. Thus, it is likely that factors other than insertion size also influence expression of these mutant alleles.

Several of the structural changes associated with the otu^{P} deletion derivatives involve the loss of regulatory regions. In the case of the DIF deletion derivatives $otu^{P\Delta2}$ and $otu^{P\Delta5}$, the upstream regulatory sequences and minor transcription start sites are intact, but the major transcription start sites, untranslated leader sequences and translation start site are deleted. Despite these alterations, both otu isoforms are detectable in these mutants, and although the level of expression is lower than in wild type, it is sufficient to produce a DIF phenotype. On the other hand, loss of upstream regulatory sequences has a more pronounced effect as demonstrated by the further reduction in expression observed in the $otu^{P\Delta3}$ ONC allele. While the level of expression in the $otu^{P\Delta6}$ QUI allele was not determined for technical reasons, the increased severity of the phenotype suggests that the loss of additional upstream sequences further reduces expression.

The deletion in $otu^{P\Delta4}$ removes the entire upstream regulatory region and extends well into the protein coding region. Considering the combined effect of losing both regulatory and coding sequences, this allele can be considered equivalent to the true null allele, $otu^{P\Delta1}$, which has lost all of the protein coding region. Thus, there is no *otu* expression in mutants carrying these QUI alleles.

The level of *otu* expression correlates with the severity of the mutant phenotype: In the QUI mutants examined, there is little or no *otu* expression as measured directly by Western analysis for the otu^{P1} allele or as inferred from the structural defects in the $otu^{P\Delta1}$ and $otu^{P\Delta4}$ alleles. The predominant type of ovariole produced by these alleles is quiescent (Table 1). From our morphological analysis it is clear that even in the absence of *otu* expression, ovarioles containing tumorous chambers are generated. The observation that germ-line derived cells are capable of proliferating in the absence of *otu* function suggests that *otu* is not absolutely required for proliferation. However, the following observations suggest that *otu* function is needed for efficient germ cell proliferation. First, ONC alleles, such as otu^{P2} and $otu^{P\Delta3}$, that express slightly higher levels of *otu* than the QUI mutations, give rise to a higher proportion of tumorous chambers. This indicates that the choice between a quiescent and tumorous pathway is affected by the

level of *otu* function. Furthermore, the dynamics of the formation of the tumorous chambers in the QUI and ONC alleles are quite different. The ovarioles from the $otu^{P\Delta 3}$ ONC allele are primarily tumorous at the time of eclosion, and the tumorous chambers continue to grow larger over time. In contrast, tumorous ovarioles are rarely observed in recently eclosed QUI mutants such as $otu^{P\Delta 1}$, but the number of tumorous ovarioles increases as the flies age (G. SASS, unpublished observation). In addition, within the population of ovarioles classified as quiescent, there appears to be a shift from agametic germaria to tumorous germaria as flies age. Such an effect of age as well as temperature on the phenotypes of EMS-induced *otu* mutations has been described previously by KING *et al.* (1986). The apparent decrease in the severity of the QUI phenotype in older flies might reflect the accumulation of a germ cell population which is proliferating at a reduced rate due to the absence of otu protein.

The low level of expression in ONC alleles can stimulate germ cell proliferation, but is not sufficient to generate a normal sixteen-cell syncytium. Uncontrolled proliferation produces tumorous chambers filled with undifferentiated germ cells resembling cystocytes. Occasionally, germ cells within a tumorous chamber display characteristics of differentiated nurse cells. DIF mutants often produce chambers which are not tumorous but that contain abnormal numbers of cystocytes. Despite the absence of a normal sixteen-cell syncytium, these cystocytes can enter the nurse cell differentiation pathway, developing into pseudo-nurse cells. A less severe DIF phenotype is characterized by a high percentage of chambers that contain both nurse cells and an oocyte, and these are often capable of developing to advanced stages of oogenesis. For example, the DIF allele otu^{P4} generates chambers with apparently normal nurse cell/oocyte syncytia, yet these cannot complete oogenesis. On the other hand, in the otu^{P3} DIF mutant, such egg chambers are capable of completing oogenesis. Our analysis of the morphologies and expression levels of DIF mutants suggests that the severity of the DIF phenotype also correlates with the level of *otu* function.

An alternative role for *otu* in oogenesis: From the analysis of mutations at the *otu* gene, it is clear that its function is required for several different events in the process of oogenesis. The above discussion suggests a direct role for *otu* in controlling proliferative and differentiation events. However, evidence from other laboratories suggests that *otu* may function in germline sex determination (PAULI and MAHOWALD 1990). The loss of proliferative control which generates a tumorous chamber might reflect a failure to receive proper sex determinative signals early in oogenesis. A similar ovarian tumor phenotype is seen in certain mutant alleles of *Sex-lethal* and *sans fille*, genes that are known to function in somatic sex determination (SCHÜPBACH 1985; GOLLIN and KING 1981; SALZ 1992). The resulting tumorous chambers in these mutants have been found to express male-specific genes and contain cells that resemble spermatocytes (STEINMANN-ZWICKY, SCHMID and NÖTHIGER 1989). One distinction between *otu* and other "ovarian tumor" genes is that *otu* mutations produce not only tumors, but also QUI and DIF chambers. In the case of QUI alleles, chamberless ovarioles may be the consequence of germ cell death due to an incompatibility between improperly determined germ cells and the female soma (OLIVER, PERRIMON and MAHOWALD 1987). However, it is difficult to envision how a defect in germ-line sex determination could produce mutants like otu^{P4}, with well developed egg chambers in which nurse cells fail to complete the transfer of their cytoplasm to the oocyte (G. SASS, unpublished observations). Thus, if *otu* is involved in signal transduction during germ-line sex determination, it may also function in other signalling events occurring both early and late in oogenesis. Regardless of how *otu* functions in the process of oogenesis, this study demonstrates that the ovarian morphologies seen in *otu* mutants can be explained as a direct consequence of altered levels of *otu* expression.

We dedicate this work to the memory of LAURA J. KALFAYAN who died May 9, 1990. The molecular characterization of the mutants described in this paper was initiated under her direction. We thank P. PUKKILA, G. MARONI, M. PEIFER and R. SWANSTROM for critical readings of this manuscript, A. COMER, W. STEINHAUER and C. KNECHT for their helpful comments, BOB KING for discussions of the *otu* mutant phenotypes, and S. WHITFIELD for art work. This work was supported by grant NP-657 from the American Cancer Society and grant DMB-9004708 from the National Science Foundation.

LITERATURE CITED

COMER, A. R., L. L. SEARLES and L. J. KALFAYAN, 1992 Identification of a genomic DNA fragment containing the *Drosophila melanogaster ovarian tumor* gene (*otu*) and localization of regions governing its expression. Gene **118:** 171–179.

BIGGIN, M. D., and R. TJIAN, 1988 Transcription factors that activate the *Ultrabithorax* promoter in developmentally staged extracts. Cell **53:** 699–711.

FEINBERG, A. P., and B. VOGELSTEIN, 1983 A technique for radiolabelling DNA restriction endonuclease fragments to high specific activity. Anal. Biochem. **132:** 6–13.

GEYER, P. K., K. L. RICHARDSON, V. G. CORCES and M. M. GREEN, 1988 Genetic instability in *Drosophila melanogaster*: *P*-element mutagenesis by gene conversion. Proc. Natl. Acad. Sci. USA *85:* 6455–6459.

GOLLIN, S. M., and R. C. KING, 1981 Studies on *fs*(1)1621, a mutation producing ovarian tumors in *Drosophila melanogaster*. Dev. Genet. **2:** 203–218.

KING, R. C., and S. F. RILEY. 1982 Ovarian pathologies generated by various alleles of the *otu* locus in *Drosophila melanogaster*. Dev. Genet. **3:** 69–89.

KING, R. C., and P. D. STORTO, 1988 The role of the *otu* gene in Drosophila oogenesis. Bioessays **8:** 18–24.

KING, R. C., D. MOHLER, S. F. RILEY, P. D. STORTO and P. S. NICOLAZZO, 1986 Complementation between alleles at the *ovarian tumor* locus of *Drosophila melanogaster*. Dev. Genet. **7:** 1–20.

KREITMAN, M., and L. F. LANDWEBER, 1989 A strategy for producing single-stranded DNA in the polymerase chain reaction: a direct method for genomic sequencing. Gene Anal. Tech. **6:** 84–88.

LINDSLEY, D. L., and G. C. ZIMM, 1992 *The Genome of Drosophila melanogaster*. Academic Press, San Diego.

MANIATIS, T., E. F. FRITSCH and J. SAMBROOK, 1982 *Molecular Cloning: A Laboratory Manual*. Cold Spring Harbor Laboratory, Cold Spring Harbor, NY

MELTON, D. A., P. A. KRIEG, M. R. REBAGLIATI, T. MANIATIS, K. ZINN and M. R. GREEN, 1984 Efficient *in vitro* synthesis of biologically active RNA and RNA hybridization probes from plasmids containing a bacteriophage SP6 promoter. Nucleic Acids Res. **12:** 7035–7056.

MULLIGAN, P. K., J. D. MOHLER and L. J. KALFAYAN, 1988 Molecular localization and developmental expression of the *otu* locus of *Drosophila melanogaster*. Mol. Cell. Biol. **8:** 1481–1488.

O'CONNELL, L. P., and M. ROSBASH, 1984 Sequence, structure, and codon preference of the Drosophila *ribosomal protein 49* gene. Nucleic Acids Res. **12:** 5495–5513.

O'HARE, K., and G. M. RUBIN, 1983 Structures of *P* transposable elements and their sites of insertion and excision in the *Drosophila melanogaster* genome. Cell **34:** 25–35.

OLIVER, B., N. PERRIMON and A. P. MAHOWALD, 1987 The *ovo* locus is required for sex-specific germ line maintenance in Drosophila. Genes Dev. **1:** 913–923.

PAULI, D., and A. P. MAHOWALD, 1990 Germ-line sex determination in *Drosophila melanogaster*. Trends Genet. **6:** 259–264.

PERKINS, K. K., G. DAILEY and R. TJIAN, 1988 *In vitro* analysis of the *Antennapedia* P2 promoter: identification of a new Drosophila transcription factor. Gene Dev. **2:** 1615–1626.

PTASHNE, M. 1986 Gene regulation by proteins acting nearby and at a distance. Nature **322:** 697–701.

SAIKI, R. K., S. SCHARF, F. FALOONA, K. B. MULLIS, G. T. HORN, H. A. ERLICH and N. ARNHEIM, 1985 Enzymatic amplification of β-globin sequences and restriction site analysis for diagnosis of sickle cell anemia. Science **230:** 1450–1354.

SALZ, H. K., 1992 The genetic analysis of *snf*: a Drosophila sex determination gene required for activation of *Sex-lethal* in both the germline and the soma. Genetics **130:** 547–554.

SANGER, F., S. NICKLEN and A. R. COULSON, 1977 DNA sequencing with chain-terminating inhibitors. Proc. Natl. Acad. Sci. USA **74:** 5463–5467.

SCAVARDA, N. J., and D. L. HARTL, 1984 Interspecific DNA transformation in Drosophila. Proc. Natl. Acad. Sci. USA **81:** 7515–7519.

SCHÜPBACH, T., 1985 Normal female germ cell differentiation requires the female *X*-chromosome to autosome ratio and expression of *Sex-lethal* in *Drosopohila melanogaster*. Genetics **109:** 529–548.

SPRADLING, A., 1992 Developmental genetics of oogenesis, in *Drosophila Development*, edited by M. BATE and A. MARTINEZ-ARIAS. Cold Spring Harbor Laboratory, Cold Spring Harbor, N.Y. (in press).

STEINHAUER, W. R., and L. J. KALFAYAN, 1992 A specific *ovarian tumor* protein isoform is required for efficient differentiation of germ cells in *Drosophila melanogaster*. Genes Dev. **6:** 233–243.

STEINHAUER, W. R., R. C. WALSH and L. J. KALFAYAN, 1989 Sequence and structure of the *Drosophila melanogaster ovarian tumor* gene and generation of an antibody specific for the ovarian tumor protein. Mol. Cel. Biol. **9:** 5726–5732.

STEINMANN-ZWICKY, M., H. SCHMID and R. NÖTHIGER, 1989 Cell-autonomous and inductive signals can determine the sex of the germ line of Drosophila by regulating the gene *Sxl*. Cell **57:** 157–166.

STORTO, P. D., and R. C. KING, 1987 Fertile heteroallelic combinations of mutant alleles of the *otu* locus of *Drosophila melanogaster*. Roux's Arch. Dev. Biol. **196:** 210–221.

STORTO, P. D., and R. C. KING, 1988 Multiplicity of functions for the *otu* gene products during Drosophila oogenesis. Dev. Genet. **9:** 91–120.

WAKIMOTO, B. T., L. J. KALFAYAN and A. C. SPRADLING, 1986 Developmentally regulated expression of Drosophila chorion genes introduced at diverse chromosomal positions. J. Mol. Biol. **187:** 33–45.

WILLIAM, J. A., S. S. PAPPU and J. B. BELL, 1988 Molecular analysis of hybrid dysgenesis-induced derivatives of a *P*-element allele at the *vg* locus. Mol. Cell. Biol. **8:** 1489–1497.

Communicating editor: M. J. SIMMONS